



Supplement of

High-resolution topography of the Antarctic Peninsula combining the TanDEM-X DEM and Reference Elevation Model of Antarctica (REMA) mosaic

Yuting Dong et al.

Correspondence to: Ji Zhao (zhaoji@cug.edu.cn)

The copyright of individual parts of the supplement might differ from the article licence.

Table S1. Literature review of existing DEM products covering Antarctica or Antarctic Peninsula

DEM product	Coverage	Data source	Temporal coverage	Posting	Absolute vertical accuracy
RAMPv2 DEM (Liu et al. 2001)	Antarctica 60° S–90° S	cartographic data; remotely sensed data; survey data	1 January 1940 to 1 January 1999	1 km, 400 m, 200 m	Rugged mountainous areas: 100 m; Steeply sloped coastal regions: 15 m; Ice shelves: 1 m; Gently sloping interior ice sheet: 7.5 m
GLAS/ICESat 500 m					
Laser Altimetry DEM of Antarctica (DiMarzio et al. 2007)	Antarctica 63° S–86° S	GLAS/ICESat laser altimetry profile data	1 February 2003 to 30 June 2005	500 m	Ranging from less than 1m to tens of meters
New 1km DEM of Antarctica from combined radar and laser data (Bamber et al. 2009; Griggs and Bamber 2009)					
	Antarctica North of 90° S	ERS-1 radar and GLAS/ICESat laser altimetry data	ERS-1 RA data: 1991 to May 1995; GLAS/ICESat data: February 2003 to March 2008	1 km	Ice shelves: 1 m; Grounded ice sheet: 2 m – 6m; Steep sloping margins: greater than 20 m.
SPOT 5 Reference Images and Topographies (SPIRIT) DTM (Korona et al. 2009)	Selected polar regions at 81.15° N–81.15° S	SPOT 5 stereoscopic images	July 2007 to April 2008	40 m	6 m
ASTER GDEM (Abrams et al. 2020; ASTER GDEM Validation Team 2009, 2011)					
	Global DEM 83° N–83° S	visible and near- infrared satellite data	March 2000 to November 2007	30 m	10 m
Improved ASTER GDEM	Antarctic Peninsula	ASTER GDEM	March 2000 to November 2007	100 m	4 m

(Cook et al. 2012)	63° S–70° S					
Bedmap2, surface DEM (Fretwell et al. 2013)	Antarctica 60° S–90° S	ASTER GDEM, SPIRIT DTM, satellite radar and laser altimetry data, the Ohio State University DEM	The vast majority of data were collected in the last two decades	1 km	30 m (rising to 130 m over mountains)	
CryoSat-2 Antarctic DEM 2012 (Helm et al. 2014)	Antarctica North of 90° S	CryoSat-2 satellite radar altimetry data	January 2012 to January 2013	1 km	90 % of the area of ice sheets: 3 m ± 15 m.	
CryoSat-2 Antarctic DEM 2017 (Fei et al. 2017)	Antarctica North of 90° S	CryoSat-2 satellite radar altimetry data	December 2012 to January 2015	1 km	Domes: 1 m; Ice shelves: 4 m; Interior ice sheet: 10 m; Rugged mountainous and coastal areas: 150 m.	
CryoSat-2 Antarctic DEM 2018 (Slater et al. 2018)	Antarctica North of 88° S	CryoSat-2 satellite radar altimetry data	July 2010 to July 2016	1 km	9.5 m	
Regional DEM of northern Antarctic Peninsula (Fieber et al. 2018)	Sixteen glaciers at Elephant Island, King George Island, Lindblad Cove and Anvers Island.	Stereo WorldView-2 and archival aerial imagery	Archival data acquired in austral summers of 1956 and 1957; WorldView-2 data acquired in 2013/2014	< 1 m	< 5 m	
TanDEM-X global DEM (Rizzoli et al. 2017; Wessel 2016)	Global DEM 85° N–90° S	TanDEM-X bistatic stripmap InSAR data	December 2010 to January 2015 (for global acquisitions); April to November of 2013 and 2014	12, 30 and 90 m	Overall absolute vertical accuracy: 3.49 m Greenland and Antarctica: 6.37 m	

(for acquisitions over Antarctica)						
REMA DEM (Howat et al. 2019)	Antarctica North of 88° S	submeter resolution optical, commercial satellite imagery	September 2008 to August 2014	Less than 10 m	less than 1 m	
TanDEM-X PolarDEM 90m of Antarctica (Wessel et al. 2021)	Antarctica	TanDEM-X bistatic stripmap InSAR data	April to November of 2013 and 2014, data gaps filled with acquisitions taken between July 2016 and September 2017	90 m	validation over blue ice achieved a mean vertical height error of just $-0.3m \pm 2.5m$ standard deviation.	

Table S2. Statistics of DEM height differences between the laser points and the TDM DEMs after each iteration of correction over the local sample area in Figure 11. All height units are in meters. Height differences are calculated as DEM elevation minus laser height.

Elevation Range	LVIS 2015				ATL06 2019												
	Corrected region		Entire region		Corrected region		Entire region										
	Median	RMSE	LE90	MAE	Median	RMSE	LE90	MAE									
After 1st correction	1500-2000	-0.24	10.14	17.09	6.81	1.08	8.59	12.05	5.26	-5.22	17.51	27.12	11.80	-2.47	15.57	22.29	9.20
After 2nd correction	1500-2000	0.42	6.73	12.01	5.01	1.31	6.35	9.54	4.23	-3.05	6.14	11.44	5.40	-1.15	5.79	10.55	4.67
After 3rd correction	1500-2000	0.68	4.98	8.09	4.07	1.42	4.57	7.78	3.85	-2.62	4.36	7.22	4.04	-1.20	4.46	7.17	3.82

Table S3. Statistics of DEM height differences between the laser altimetry points and the corrected TDM DEMs after each iteration of correction over the Hektoria and Green Glaciers area in Figure 12. All height units are in meters. Height differences are calculated as DEM elevation minus laser height.

		LVIS 2015								ATL06 2019							
		Corrected region				Entire region				Corrected region				Entire region			
Elevation Range		Median	RMSE	LE90	MAE	Median	RMSE	LE90	MAE	Median	RMSE	LE90	MAE	Median	RMSE	LE90	MAE
After 1st correction	15-2200	5.72	23.17	39.04	16.31	3.46	19.43	32.81	12.37	2.99	21.38	32.79	15.94	-1.37	15.27	24.53	10.05
	15-500	5.64	15.23	31.21	11.83	5.71	14.52	29.67	11.20	5.93	16.59	30.53	14.21	1.58	15.53	28.50	12.26
	500-1000	11.40	23.89	39.66	19.66	5.01	19.44	33.69	13.84	2.50	17.34	27.07	13.79	0.58	11.34	18.10	8.05
	1000-1500	7.73	36.93	55.17	25.16	3.48	28.33	40.53	16.78	1.38	41.43	56.77	24.62	-2.56	20.07	16.53	10.09
	1500-2000	-18.71	29.79	48.20	27.34	-2.19	20.30	41.05	12.05	-28.45	23.79	52.71	32.38	-4.30	15.20	26.41	9.87
	2000-2200	-18.22	16.86	44.47	22.41	0.03	10.13	14.08	5.45	-65.74	0.94	65.92	65.19	-5.72	6.18	9.16	6.23
After 2nd correction	15-2200	2.54	11.81	15.52	8.06	2.06	10.29	13.80	6.86	-1.89	11.87	18.28	9.28	-2.49	9.11	14.55	7.02
	15-500	3.08	8.23	12.76	6.38	3.42	8.05	12.68	6.36	0.78	10.71	17.17	8.57	-1.23	9.84	16.26	7.78
	500-1000	2.32	13.13	18.03	9.07	2.95	10.94	14.98	7.33	-5.17	10.44	16.91	8.28	-1.75	8.23	10.95	6.25
	1000-1500	2.87	21.48	26.02	13.11	2.11	17.07	19.76	9.90	0.26	18.14	31.11	13.12	-2.77	10.27	12.95	7.59
	1500-2000	-7.61	14.88	18.90	11.67	-1.61	9.83	13.35	6.46	-15.17	11.42	27.23	16.31	-4.09	8.00	15.75	6.96
	2000-2200	-10.62	8.51	18.47	11.44	0.06	5.66	9.95	3.85	-41.93	0.94	42.10	41.37	-5.72	4.18	9.16	6.01
After 3rd correction	15-2200	1.12	10.86	13.27	6.90	1.32	9.65	12.27	6.15	-3.68	10.84	17.61	8.74	-3.06	8.59	14.40	6.82
	15-500	1.99	7.75	11.76	5.68	2.40	7.69	11.88	5.76	-0.59	10.12	17.18	7.91	-1.88	9.29	16.23	7.27
	500-1000	0.00	11.65	15.03	7.36	1.87	10.10	12.66	6.32	-7.39	9.60	17.32	9.11	-3.33	8.32	11.44	6.57
	1000-1500	0.56	20.67	24.28	11.40	1.22	16.60	18.44	9.04	-1.38	12.39	14.30	8.72	-2.83	8.35	11.43	6.72
	1500-2000	-6.40	13.21	13.98	9.70	-1.68	9.03	11.51	5.94	-13.00	10.57	20.32	13.54	-4.11	7.41	15.00	6.60
	2000-2200	-8.68	6.81	12.59	8.72	0.01	5.01	8.82	3.63	-41.72	0.90	42.14	41.37	-5.59	4.34	8.97	5.94

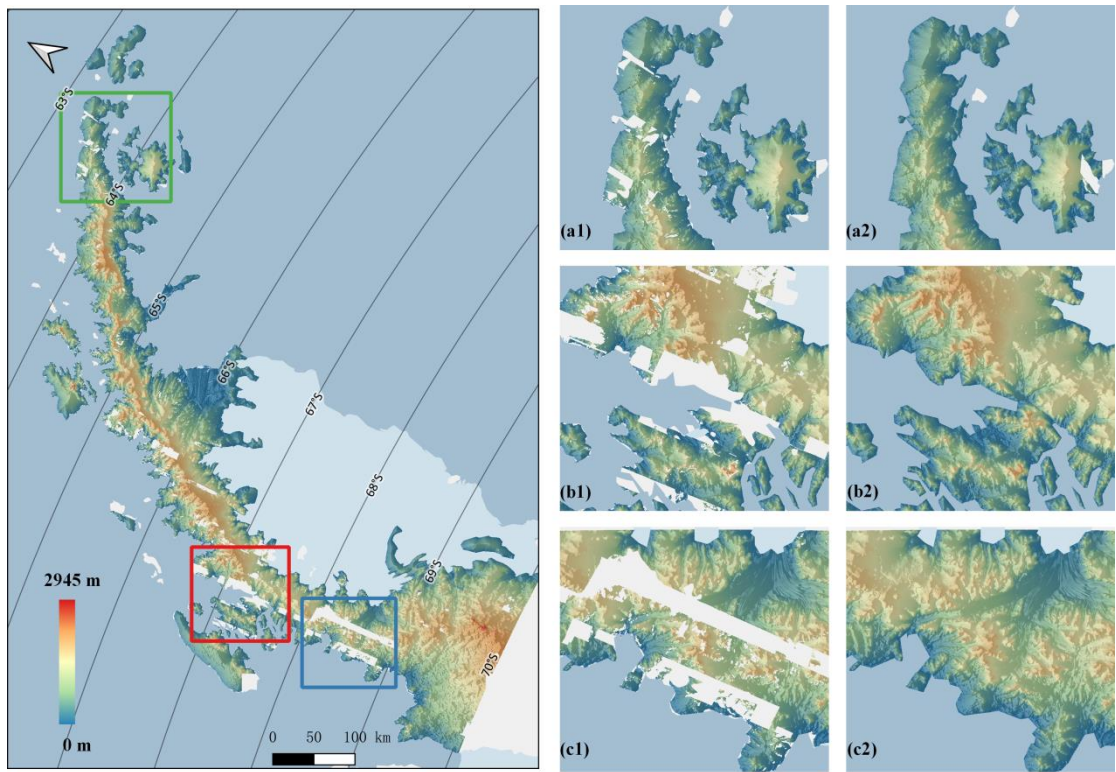


Figure S1 REMA mosaic covering AP with three sample areas. Right panel: detailed comparison of the REMA mosaic (left column) and TDM DEM (right column) at the sample areas.

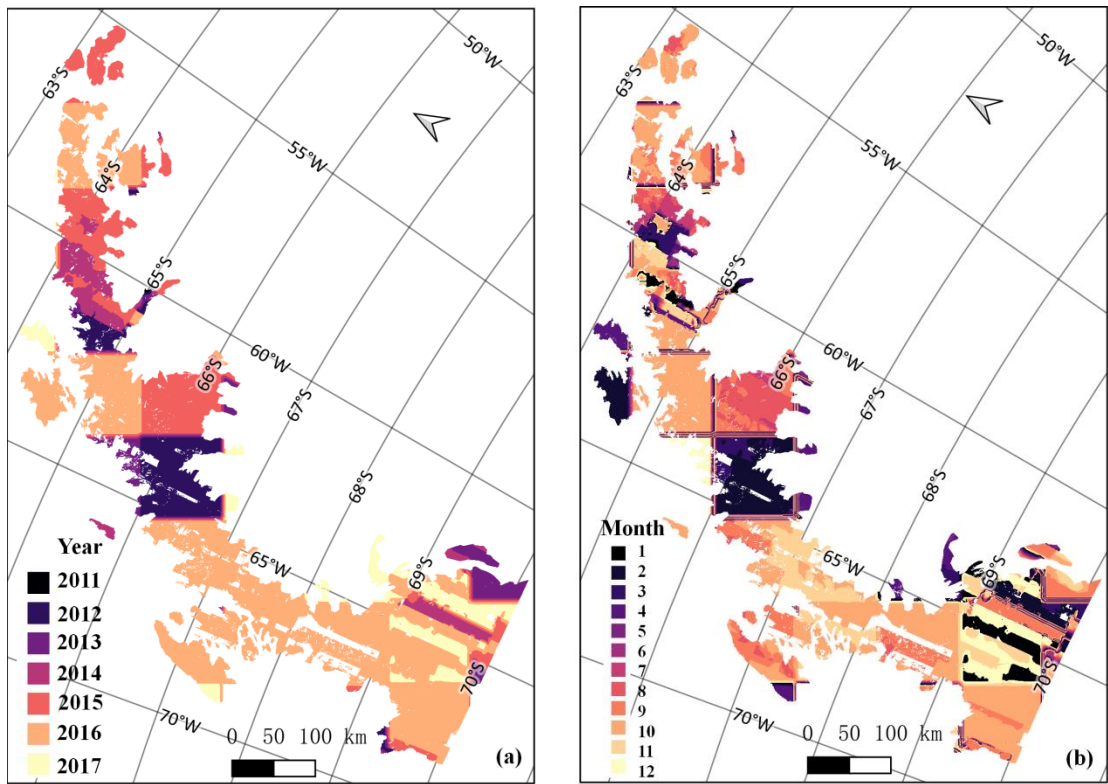


Figure S2 Acquisition time in (a) year and (b) month of REMA mosaic covering AP.

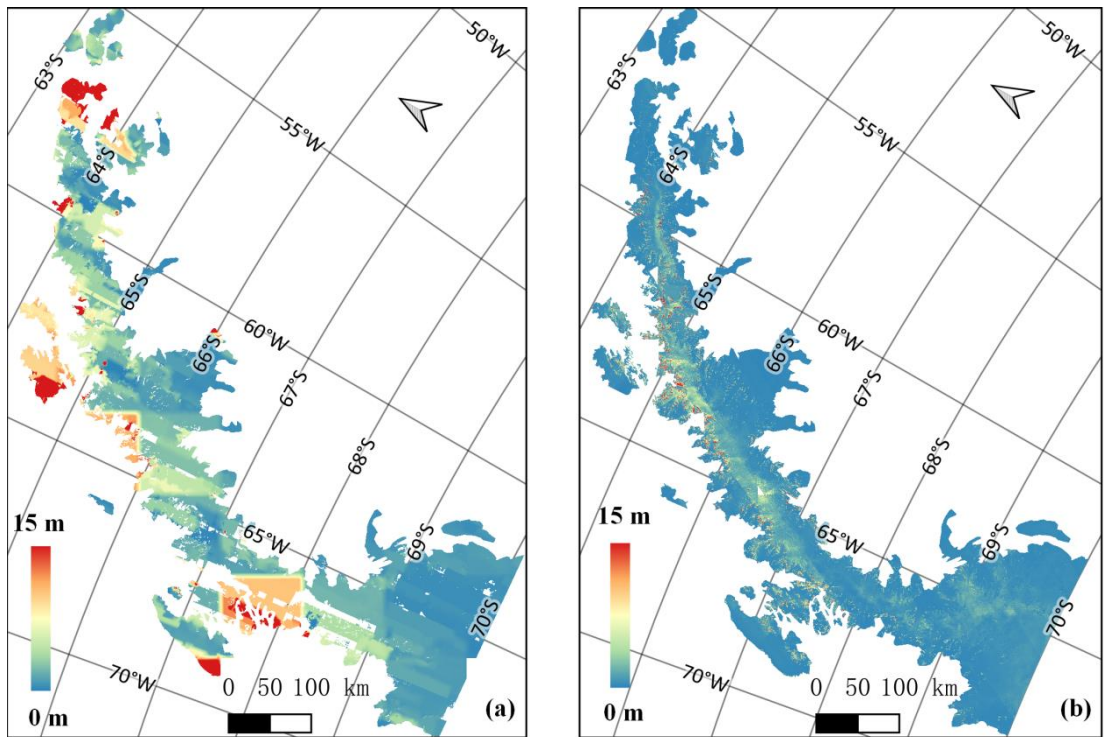


Figure S3 Random elevation errors of (a) REMA mosaic and (b) TDM DEM covering AP.

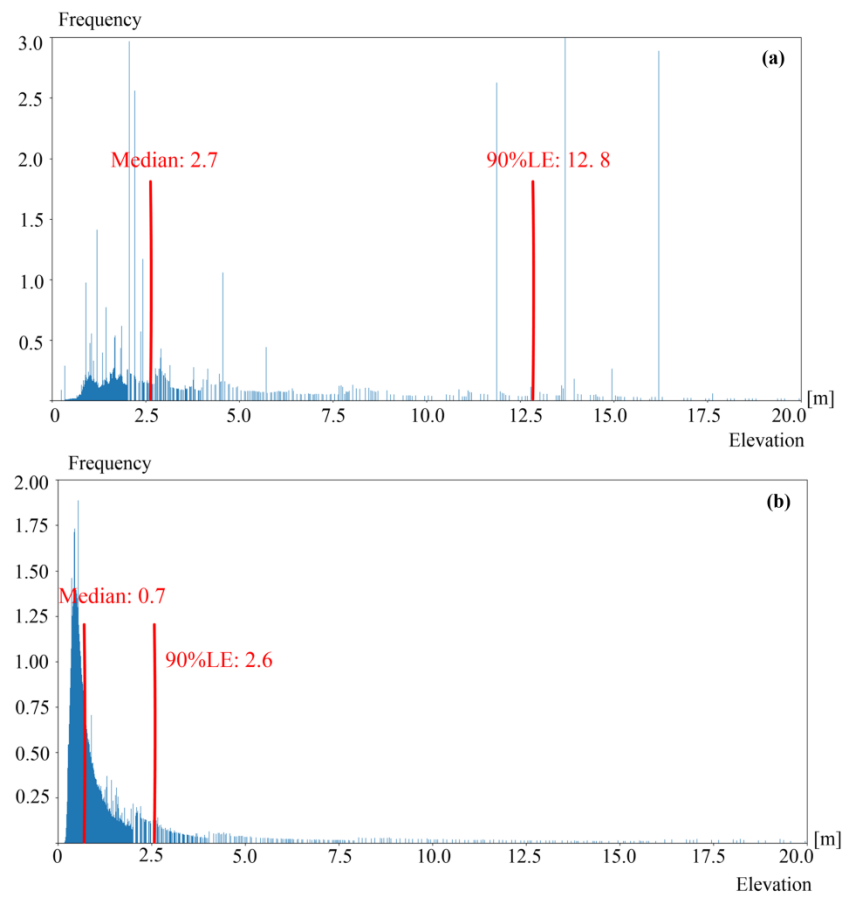


Figure S4 Histograms of random elevation errors of (a) REMA mosaic and (b) TDM DEM covering AP. Median value and 90% quantile of the errors (90%LE) are marked in red in the histograms.

References

- Abrams, M., Crippen, R., and Fujisada, H.: ASTER Global Digital Elevation Model (GDEM) and ASTER Global Water Body Dataset (ASTWBD), *Remote Sens.*, 12(7), 1156; <https://doi.org/10.3390/rs12071156>, 2020.
- ASTER GDEM Validation Team: ASTER Global Digital Elevation Model Version 2 – Summary of Validation Results, NASA Land Processes Distributed Active Archive Center and Joint Japan-US ASTER Science Team, available at: http://www.jspacesystems.or.jp/ersdac/GDEM/ver2Validation/Summary_GDEM2_validation_report_final.pdf (last access: 3 September 2021), 2009.
- ASTER GDEM Validation Team: METI/ERSDAC, NASA/LPDAAC, USGS/EROS, in cooperation with NGA and other collaborators, ASTER GDEM Validation Summary Report, available at: https://lpdaac.usgs.gov/documents/28/ASTER_GDEM_Validation_1_Summary_Report.pdf (last access: 3 September 2021), 2011.
- Bamber, J. L., Gomez-Dans, J. L., and Griggs, J. A.: A new 1 km digital elevation model of the Antarctic derived from combined satellite radar and laser data – Part 1: Data and methods, *The Cryosphere*, 3, 101–111, <https://doi.org/10.5194/tc-3-101-2009>, 2009.
- Cook, A. J., Murray, T., Luckman, A., Vaughan, D. G., and Barrand, N. E.: A new 100-m Digital Elevation Model of the Antarctic Peninsula derived from ASTER Global DEM: methods and accuracy assessment, *Earth Syst. Sci. Data*, 4, 129–142, <https://doi.org/10.5194/essd-4-129-2012>, 2012.
- DiMarzio, J., Brenner, A., Schutz, R., Shuman, C., and Zwally, H.: GLAS/ICESat 500 m laser altimetry digital elevation model of Antarctica, version 1. Boulder, Colorado USA, National Snow and Ice Data Center, Distributed Archive Center, <https://doi.org/10.5067/K2IMI0L24BRJ>, 2007.
- Li, F., Xiao, F., Zhang, S. K., E, D. C., Cheng, X., Hao, W. F., Yuan, L. X., and Zuo,

Y. W.: DEM development and precision analysis for Antarctic ice sheet using Cryosat-2 altimetry data, Chin. J. Geophys., 60(5), 1617–1629, <https://doi.org/10.6038/cjg20170501>, 2017.

Fieber, K. D., Mills, J. P., Miller, P. E., Clarke, L., Ireland, L., and Fox, A. J.: Rigorous 3D change determination in Antarctic Peninsula glaciers from stereo WorldView-2 and archival aerial imagery, Remote Sens. Environ., 205, 18–31, <https://doi.org/10.1016/j.rse.2017.10.042>, 2018.

Fretwell, P., Pritchard, H. D., Vaughan, D. G., Bamber, J. L., Barrand, N. E., Bell, R., Bianchi, C., Bingham, R. G., Blankenship, D. D., Casassa, G., Catania, G., Callens, D., Conway, H., Cook, A. J., Corr, H. F. J., Damaske, D., Damm, V., Ferraccioli, F., Forsberg, R., Fujita, S., Gim, Y., Gogineni, P., Griggs, J. A., Hindmarsh, R. C. A., Holmlund, P., Holt, J. W., Jacobel, R. W., Jenkins, A., Jokat, W., Jordan, T., King, E. C., Kohler, J., Krabill, W., Riger-Kusk, M., Langley, K. A., Leitchenkov, G., Leuschen, C., Luyendyk, B. P., Matsuoka, K., Mouginot, J., Nitsche, F. O., Nogi, Y., Nost, O. A., Popov, S. V., Rignot, E., Rippin, D. M., Rivera, A., Roberts, J., Ross, N., Siegert, M. J., Smith, A. M., Steinhage, D., Studinger, M., Sun, B., Tinto, B. K., Welch, B. C., Wilson, D., Young, D. A., Xiangbin, C., and Zirizzotti, A.: Bedmap2: improved ice bed, surface and thickness datasets for Antarctica, The Cryosphere, 7, 375–393, <https://doi.org/10.5194/tc-7-375-2013>, 2013.

Griggs, J. A. and Bamber, J. L.: A new 1 km digital elevation model of Antarctica derived from combined radar and laser data – Part2: Validation and error estimates, The Cryosphere, 3, 113–123, <https://doi.org/10.5194/tc-3-113-2009>, 2009.

Helm, V., Humbert, A., and Miller, H.: Elevation and elevation change of Greenland and Antarctica derived from CryoSat-2, The Cryosphere, 8, 1539–1559, <https://doi.org/10.5194/tc-8-1051539-2014>, 2014.

Howat, I. M., Porter, C., Smith, B. E., Noh, M.-J., and Morin, P.: The Reference

Elevation Model of Antarctica, The Cryosphere, 13, 665–674,
<https://doi.org/10.5194/tc-13-665-2019>, 2019.

Korona, J., Berthier, E., Bernard, M., Rémy, F., and Thouvenot, E.: SPIRIT. SPOT 5 stereoscopic survey of polar ice: reference images and topographies during the fourth International Polar Year (2007–2009), ISPRS J. Photogramm. Remote Sens., 64, 204–212, 2009.

Liu, H., Jezek, K., Li, B., & Zhao, Z: Radarsat Antarctic Mapping Project digital elevation model version 2. Boulder, Colorado USA, National Snow and Ice Data Center, Distributed Archive Center,
<https://doi.org/10.5067/8JKNEW6BFRVD>, 2001.

Rizzoli, P., Martone, M., Gonzalez, C., Wecklich, C., Tridon, D. B., Bräutigam, B., Bachmann, M., Schulze, D., Fritz, T., and Huber, M.: Generation and performance assessment of the global TanDEM-X digital elevation model, ISPRS J. Photogramm. Remote Sens., 132, 119–139, 2017.

Slater, T., Shepherd, A., McMillan, M., Muir, A., Gilbert, L., Hogg, A. E., Konrad, H., and Parrinello, T.: A new digital elevation model of Antarctica derived from CryoSat-2 altimetry, The Cryosphere, 12, 1551–1562,
<https://doi.org/10.5194/tc-12-1551-2018>, 2018.

Wessel, B., 2016. TanDEM-X Ground Segment — DEM Products Specification Document. In: Tech. rep. EOC, DLR, Oberpfaffenhofen, Germany. Public Document TD-GS-PS0021, Issue 3.1. Available:
https://elib.dlr.de/108014/1/TD-GS-PS-0021_DEM-Product-Specification_v3.1.pdf (last access: 3 September 2021), 2016.

Wessel, B., Huber, M., Wohlfart, C., Bertram, A., Osterkamp, N., Marschalk, U., Gruber, A., Reuß, F., Abdullahi, S., Georg, I., and Roth, A.: TanDEM-X PolarDEM 90 m of Antarctica: Generation and error characterization, The Cryosphere Discuss. [preprint], <https://doi.org/10.5194/tc-2021-19>, in review, 2021.